

²Weber, R. and Brauchli, H., "Dynamics of a System of Two Satellites Connected by a Deployable and Extensible Tether of Finite Mass," Vols. I & II, ETH, Swiss Federal Inst. of Technology, Zurich, Switzerland, Rept. ESTEC Contract 2992/76/NL/AK(SC), 1978.

³Misra, A. K., and Modi, V. J., "A General Dynamical Model for the Space Shuttle Based Tethered Satellite System," *Advances in the Astronautical Sciences*, Vol. 40, Part II, 1979, pp. 537-557.

⁴Baker, W. P., Dunkin, J. A., Galaboff, A. J., Johnston, K. D., Kissel, R. R., Rheinfurth, M. H., and Seibel, M. P. P., "Tethered Subsatellite Study," NASA TM X-73314, March 1976.

⁵Liangdong, L., and Bainum, P. M., "Effect of Tether Flexibility on the Tethered Shuttle Subsatellite Stability and Control," *Journal of Guidance, Control, and Dynamics*, Vol. 12, No. 6, 1989, pp. 866-873.

⁶von Flotow, A. H., and Williamson, P. R., "Fast (3/4 Orbit) Deployment of a Tethered Satellite Pair to the Local Vertical," NASA/AIAA/PSN International Conf. on Tethers in Space, Arlington, VA, Sept. 17-19, 1986.

⁷Kane, T. R., and Levinson, D. A., *Dynamics*, McGraw-Hill, New York, 1985.

⁸Kane, T. R., and Levinson, D. A., "Formulation of Equations of Motion for Complex Spacecraft," *Journal of Guidance and Control*, Vol. 3, No. 2, 1980, pp. 99-112.

⁹Baumgarte, J., "Stabilization of Constraints and Integrals of Motion," *Computer Methods in Applied Mechanics and Engineering*, Vol. 1, 1972, pp. 1-16.

¹⁰Wang, J. T., and Huston, R. L., "Kane's Equations with Underdetermined Multipliers—Application to Constrained Multibody Systems," *Journal of Applied Mechanics*, Vol. 54, June 1987, pp. 424-429.

Analysis of an Onboard Antenna Pointing Control System

Yoichi Kawakami,* Hiroshi Hojo,†
and Masazumi Ueba†

*Nippon Telegraph and Telephone Corporation
Radio Communication Systems Laboratories,
Yokosuka-shi, Kanagawa, Japan*

Nomenclature

- f_a = antenna drive control frequency
 I_a = moment-of-inertia of antenna reflector
 K_b = antenna drive ratio = antenna beam angle/reflector drive angle
 q = modal coordinate of antenna structures
 r = equivalent drive angle factor-reflector drive angle/reflector displacement
 T_{ac} = antenna drive control torque
 ζ_a = damping ratio of antenna support boom
 θ_a = antenna drive angle
 θ_p = antenna pointing error
 ϕ_a, ϕ'_a = modal displacement and slope, respectively, of antenna support boom
 ω_m = maximum satellite attitude rate
 ω_n = eigenfrequency of antenna support boom

Introduction

IN the 1990s multibeam satellite communications systems must be developed to achieve larger transmission capacity. To establish these systems, large onboard antennas with high

pointing accuracy are needed. In order to satisfy the requirements for high accuracy, new onboard control systems are being closely studied around the world.

In Japan, a field experiment of multibeam satellite communications is scheduled to be performed in conjunction with the sixth Japanese Engineering Test Satellite (ETS-VI), to be launched in 1992. ETS-VI is a two-ton class, three-axis stabilized geostationary satellite. The antenna pointing control systems on ETS-VI are now being designed. For this, the influence of dynamics on flexible structures must be considered. This paper describes significant system design parameters and relations between these values in the design of an onboard antenna pointing control system for ETS-VI.

System Configuration

The configuration of the onboard antenna pointing control system mounted on ETS-VI is shown in Fig. 1. An antenna drive control system (ADCS) is added to a conventional attitude control system (ACS). The ADCS consists of an rf sensor, an antenna pointing mechanism (APM), and antenna pointing control electronics (APE). The most important function of the ADCS is to point an antenna beam in the direction of a beacon transmitted from an Earth station and thereby minimize pointing errors residual in the antenna structures and the ACS. Since the rf sensor consists of a sensor feed and a reflector in common with the communications system, pointing errors of the reflector can be easily detected. An antenna beam can be shifted individually in orbit by rotating the subreflector with the APM.

Drive Methods

Two methods of antenna pointing control are currently used: a main-reflector drive and a subreflector drive. The main-reflector drive is electrically superior to the subreflector drive for yielding less antenna gain loss and lower sidelobe. This method, however, is mechanically inferior because of high inertial load and lower eigenfrequencies. Assuming that sinusoidal satellite attitude changes generate control errors in the antenna drive control, the pointing control error e can be represented as follows:

$$e = \omega_m / 2\pi f_a \quad (1)$$

Figure 2 gives the relationship between maximum permissible pointing control error as a function of control frequency for three satellite attitude rates. The control frequency is limited to about one-tenth of the eigenfrequency of the antenna reflector that is driven, to prevent the antenna structures from resonating. In our preliminary assessment of the structures, eigenfrequencies of the main reflector and the subreflector are about 2 and 10 Hz, respectively. As the maximum attitude rate of a two-ton class satellite is about 0.001 deg/s, the subreflector drive is preferable in order to achieve a pointing control accuracy of 0.001 deg.

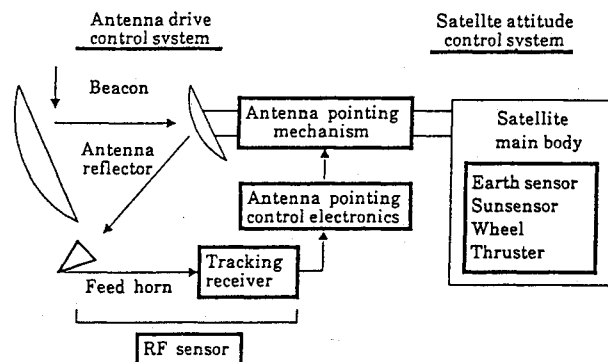


Fig. 1 Configuration of the antenna pointing control system.

Received Aug. 2, 1988; presented as Paper 88-4306 at the AIAA/AAS Astrodynamics Conference, Minneapolis, MN, Aug. 15-17, 1988; revision received March 31, 1989. Copyright © 1989 by the American Institute of Aeronautics and Astronautics, Inc. All rights reserved.

*Senior Research Engineer. Member AIAA.

†Research Engineer.

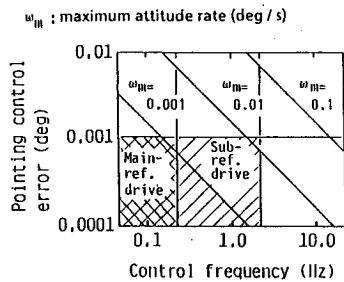


Fig. 2 Control regions of two reflector drive methods.

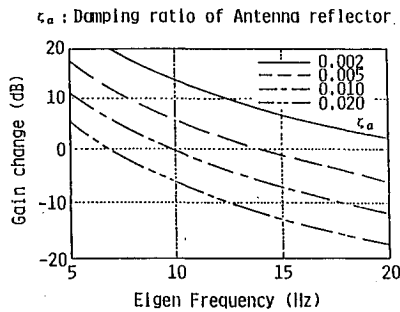


Fig. 3 Relations between control gain change and structural parameters.

Antenna Structure Dynamics

Large onboard antennas, which are stowed during launch, are deployed once the satellite reaches its designated orbit. Reflectors are supported with antenna support booms and deployment mechanisms. For satellite communications using the Ka or Ku band, the subreflector itself is rigid in comparison with the drive control frequency. However, the antenna support booms with deployment mechanisms are flexible. The antenna structures, therefore, can be modeled as a flexible cantilever with a rigid mass and a torque actuator at its tip. To prevent these structures from resonating, their eigenfrequencies must be greater than the control frequency of the ADCS. On the other hand, very high eigenfrequencies require the structure mass to be increased. To optimize the system, it is important to identify clearly the dynamics of these structures. In this study, the influences of structural parameters on control gain of the ADCS are assessed for the gain stabilization control concept.

Satellite dynamics can be ignored in the antenna pointing control system of ETS-VI because the attitude control frequency is lower than one-tenth of the antenna drive control frequency and the inertia of the satellite main body is much larger than that of the driven subreflector. The dynamics of the antenna structures, therefore, are given by

$$I_a \ddot{\theta}_a + I_a \phi_a' \ddot{q} = T_{ac} \quad (2)$$

$$I_a \phi_a' \ddot{\theta}_a + m \ddot{q} + 2\zeta_a \omega_n \dot{q} + \omega_n^2 q = 0 \quad (3)$$

$$\theta_p = K_b (\theta_a + \phi_a' q + r \phi_a q) \quad (4)$$

where $m = 1 + I_a \phi_a'^2 + m_a \phi_a^2$, in which m_a is a mass that is driven. The transfer function of these structures, $G_p(s)$, is derived using Eqs. (2-4).

$$G_p(s) = \frac{K_b}{I_a s^2} \frac{bs^2 + 2\zeta_a \omega_n s + \omega_n^2}{as^2 + 2\zeta_a \omega_n s + \omega_n^2} \quad (5)$$

where

$$a = \frac{1 + m_a \phi_a^2}{m} \quad (6a)$$

$$b = \frac{1 + m_a \phi_a^2 - I_a \phi_a' r \phi_a}{m} \quad (6b)$$

In Eq. (5), the term in parentheses represents the flexibility of the antenna structures. The gain at the eigenfrequency of the structures, $\omega_n/a^{1/2}$, is given by

$$G = \frac{K_b a [a(1 - b/a)^{1/2} + 4\zeta_a^2]}{I_a \omega_n^2 4\zeta_a^2} \quad (7)$$

To maintain sufficient gain margin in the ADCS at the resonant frequency, gain changes due to deviations in structural parameters are calculated. Figure 3 shows gain changes vs eigenfrequencies for four damping ratios. In our assessment, the nominal value of Z_a is 0.01, and its tolerance is about 0.005. The gain change is, therefore, calculated to be about 6 dB. Other flexible parameters, modal slope and modal displacement angle, were estimated in a similar manner. The control gain changes due to these tolerances were clarified as about 3 and 2 dB, respectively. As a result, a gain margin of more than 11 dB is required to make the control system stable against changes in the structural parameters.

Conclusion

Significant structural parameters of the onboard antenna pointing control system for ETS-VI were clarified, and the following conclusions were reached.

- 1) A subreflector drive is preferable to a main-reflector drive, because of required control accuracy and total antenna mass.
- 2) A control gain margin of about 11 dB is necessary for the control system to be stabilized against changes in the structural parameters.

Calculation of Stability Derivatives for Slender Bodies Using Boundary Element Method

Shinji Suzuki* and Kizuki Fukuda†
University of Tokyo, Tokyo, Japan

Introduction

THIS Note presents the application of the boundary element method to calculate the stability derivatives for a slender body. Aerodynamic characteristics of slender fuselages, wings, and their combinations have been estimated using the slender-body theory in the initial design stage.¹ This theory can transform three-dimensional flow problems into two-dimensional, incompressible flow problems in the cross-flow plane perpendicular to the long axis of the body.^{2,3} Bryson has shown that the theoretical stability derivatives of the slender body could be determined by use of the concept of apparent-mass coefficients of the crossflow section of the slender body.⁴ However, since the conformal mapping technique has been used to analyze the two-dimensional flow, it has been difficult to calculate the stability derivatives of a complicated configuration by the slender-body theory. In the present Note, the boundary element method⁵ is applied to

Received Oct. 4, 1988; revision received May 29, 1989. Copyright © 1989 by the American Institute of Aeronautics and Astronautics, Inc. All rights reserved.

*Associate Professor, Department of Aeronautics.

†Graduate Student, Department of Aeronautics.